Protonation and Hydrogenation Experiments with Iridium(0) and Iridium(−1) tropp Complexes: Formation of Hydrides

by **Carsten Böhler**, **Narcis Avarvari**[1], **Hartmut Schönberg**, **Michael Wörle**, **Heinz Rüegger**, and **Hansjörg Grützmacher***[2]

Laboratory of Inorganic Chemistry, ETH-Hönggerberg, CH-8093 Zürich

Dedicated to the memory of Professor *Luigi M. Venanzi*

The reactions of three different tetracoordinated Ir complexes, $[Ir(tropp^{ph})_2]^n$ ($n = +1, 0, -1$), which differ in the formal oxidation state of the metal from +1 to −1, with proton sources and dihydrogen were investigated (tropp = 5-(diphenylphosphanyl)dibenzo[*a*,*d*]cycloheptene). It was found that the cationic 16-electron complex $[Ir(tropp^{ph})_2]^+$ (**2**) cannot be protonated but reacts with $NaBH_4$ to the very stable 18-electron Ir^I hydride $[IrH(tropp^{ph})_2]$ (**5**), which is further protonated with medium strong acids to give the 18-electron Ir^{III} dihydride $[IrH_2(tropp^{ph})_2]^+$ (**6**; pK_s in CH_2Cl_2/THF/H_2O 1:1:2 *ca.* 2.2). Both, the neutral 17-electron Ir^0 complex $[Ir(tropp^{ph})_2]$ (**3**) and the anionic 18-electron complex $[Ir(tropp^{ph})_2]^-$ (**4**) react rapidly with H_2O to give the monohydride **5**. In reactions of **3** with H_2O, the terminal Ir^I hydroxide $[Ir(OH)(tropp^{ph})_2]$ (**8**) is formed in equal amounts. All these complexes, apart from **5**, which is inert, do react rapidly with dihydrogen. The complex **2** gives the dihydride **6** in an oxidative addition reaction, while **3**, **4**, and **8** give the monohydride **5**. Interestingly, a salt-type hydride (*i.e.*, LiH) is formed as further product in the unexpected reaction with $[Li(thf)_x]^+$-$[Ir(tropp^{ph})_2]^-$ (**4**). Because **3** undergoes disproportionation into **2** and **4** according to $2\,\mathbf{3} \rightleftarrows \mathbf{2} + \mathbf{4}$ ($K_{disp} = 2.7 \cdot 10^{-5}$), it is likely that actually the diamagnetic species and not the odd-electron complex **3** is involved in the reactions studied here, and possible mechanisms for these are discussed.

Introduction. – Rh and Ir complexes in their formal oxidation states of 0 and −1 have a promising potential in bond-activation chemistry (for an early report on *Reppe*-type hydroformylations with Rh^0 carbonyls, see [1]; for C−H activation, see [2]; for electrochemical CO_2 reduction with $[RhCl(dppe)_2]$, see [3]; for electrochemical CO_2 reduction with $[MCl(CO)(PPh_3)_2]$ (M = Rh,Ir), see [4]; for chemical reduction with $[BrMg]^+[Rh(Ph_2P-(Ch_2)_n-PPh_2]^-$ ($n = 2, 3$), see [5]; for hydroformylation, see [6]), and they were discussed in the context of the photocatalytic H_2O splitting in order to produce H_2 as a carrier of chemical energy (for photochemical H_2O reduction, see [7]). However, relatively little is known about mononuclear complexes containing these metal centres in such formal oxidation states. Assuming that electron-withdrawing ligands should stabilize formally low metal-oxidation states, early work focused on the synthesis of the carbonyl species $[M(CO)_4]$ and $[M(CO)_4]^-$ (M = Rh, Ir). However, the paramagnetic d^9-valence-electron-configured $[M(CO)_4]$ complexes were only observed in inert-gas matrices at very low temperatures [8–10]. On the other side, the colorless anionic d^{10}-valence-electron-configured $[M(CO)_4]^-$ ions are quite stable and were

[1] Current address: Dr. Narcis Avarvari, Institut des Matériaux Jean Rouxel, CNRS FRE 2068, 2, rue de la Houssinière – BP 32229, F-44322 Nantes Cedex 3. e-mail: narcis.avarvari@cnrs-imn.fr.

[2] Phone: +41 1 632 28 55, Fax: +41 1 632 10 90, e-mail: gruetzmacher@inorg.chem.ethz.ch.

prepared in form of various alkali metal and NH_4^+ salts ($[Rh(CO)_4]^-$: [11], $[Ir(CO_4)]^-$: [12]). When fluorophosphines like PF_3 or PF_2NMe_2 are used as electron-withdrawing ligands, a similar picture arises, *i.e.*, the complex anions $[M(PF_3)_4]^-$ (M = Rh, Ir) ($[Rh(PF_3)_4]^-$: [13], $[Rh(PF_3)_4]^-$ and $[Ir(PF_3)_4]$: [14]) or $[Rh(PF_2NMe_2)_4]$ ($[Rh(PF_2NMe_2)_4]$: [15]) are easily prepared and isolated, while the neutral $[M(PF_3)_4]$ complexes could not be characterized, and the dimers $[M_2(PF_3)_8]$ were isolated instead. Upon thermal cleavage of the dimer $[Rh_2(PF_3)_8]$, the monomeric $[Rh(PF_3)_4]$ was suggested to be the component of a deep green sublimate [14], but this complex is only stable at low temperatures. The syntheses of some stable mixed phosphine carbonyl rhodates and iridates of general type $[M(CO)_x(P)_y]^-$ ($[Rh(CO)_2(PPh_3)_2]^-$ and $[Rh(CO)_3(PPh_3)]$: [16], $[Rh(CO)(triphos)]^-$: [17]) and tetraphosphine complexes $[M(P)_4]^-$ [5] ($[Ir(dppf)_2]^n$ ($n = +1, 0, -1$; dppf = 1,1′-bis(diphenylphosphino)ferrocene): [18]) [19] (*P* stands for any ligand binding *via* a P-atom) were described but again the neutral paramagnetic 17-electron species $[M(CO)_x(P)_y]$ ($[M(CO)(PPh_3)_4]$: [20]) or $[M(P)_4]$ ($[Rh(PPh_3)_4]$): [21]; molecular dynamics and dimerization of $[Rh(dppe)_2]$: [22]) were elusive, and very mostly dimers were obtained [22] (preferred species in these systems seem to be the CO-bridged dimers like $[Rh_2(\mu_2\text{-}CO)_2(CO)_3(PR_3)_3]$ [23]; see also [24]). Exceptions are the paramagnetic 17-electron complexes $[Rh\{P(O^iPr_3\}_4]$ [25] and $[Ir(dppf)_2]$ [18] (dppf = 1,1′-bis(diphenylphosphino)ferrocene), which were obtained as deep blue or green solids, respectively.

The electrochemical generation of N-heterocyclic Rh and Ir complexes in formally low oxidation states of general formula $[M(bipy)_x(L)_y]^n$ or $[M(phen)_x(L)_y]^n$ (M = Rh, Ir, $n = 0, -1$) [26] (for a short overview about the electrochemistry and an investigation of N-heterocyclic Rh^I and Ir^I complexes, see [27]) [28], and the Rh olefin complexes $[Rh(cod)_2]^n$ ($n = 0, -1$) [29] was also intensively investigated (bipy = 2,2′-bipyridyl, phen = 1,10-phenanthroline; cod = cyclooctadiene). A common feature of these Rh and Ir $[ML_4]^n$ ($n = 0, -1$, L = any ligand) complexes in low formal oxidation states is their high reactivity against protic reagents, and the resulting hydrides $[MHL_4]$ [3][5][6][13][14][16][24] (for first characterization of $[RhH(CO)_4]$, see [30]; for an early report on $[IrH(CO)_4]$, see [31]) were sometimes isolated as the products in electrochemical reactions [20][32] ([32] cites also literature for alternative routes to prepare $[MH(P)_4]$).

We had developed the tropp ligand **1** ($tropp^{ph}$ = *trop*ylidenyl *p*hosphane; *IUPAC:* 5-(diphenylphosphanyl)dibenzo[*a*,*d*]cycloheptene; the ph in the superscript indicates the substituent bonded to the P-centre) as a new ligand system [33]. This ligand, in which a phosphine and an olefinic binding site form a rigid concave bidentate chelate structure (*Fig. 1*), allowed the synthesis and isolation of closely related d^8-, d^9-, and d^{10}-valence-electron-configured Rh [34][35] and Ir [36] $[M(tropp^{ph})_2]$ complexes, which were all characterized by X-ray analyses.

A remarkable feature of the $[M(tropp^{ph})_2]^n$ complexes are the low reduction potentials for the couples $[M(tropp^{ph})_2]^+/[M(tropp^{ph})_2]^0$ (*ca.* −1 V) and $[M(tropp^{ph})_2]^0/[M(tropp^{ph})_2]^-$ (> −1.2 V), while for other systems quite negative potentials (usually < −1.5 V) for the first reduction step and potentials close to or lower than −2 V for the second step were measured (all potentials *vs.* Ag/AgCl). The 16-electron Ir complex $[Ir(tropp^{ph})_2]^+$ **2** is reduced at especially low potentials to both the neutral d^9-**3** and the

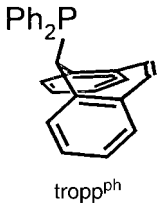

1

Fig. 1. *Graphic representation of the tropp^{ph} ligand*

anionic d^{10}-**4** compounds (see *Scheme 1*). From the redox potentials, $E^{1o}_{1/2} = -0.65$ V and $E^{2o}_{1/2} = -0.92$ V (CH_2Cl_2, Bu_4NPF_6 electrolyte) the formation constant $K_f = 3.7 \cdot 10^4$ for the reaction $[Ir(tropp^{ph})_2]^+$ **2** + $[Ir(tropp^{ph})_2]^-$ **4** $\rightleftharpoons$ 2 $[Ir(tropp^{ph})_2]$ **3** is calculated, which is also a convenient way to prepare **3**.

Results. – *Reactions with Protons or Hydrides.* Hydrides play a crucial role in any X–H activation chemistry. Furthermore, although numerous Ir hydrides were described in the literature (for a general overview of transition-metal hydrides, see [37]) [38–40], fewer reports appeared on complexes in which olefins, especially nonactivated ones, and hydrides are combined in the coordination sphere (Iridium cyclooctadiene hydrides can be prepared; however, they are usually only stable at low temperatures; see, *e.g.*, [41]) [42]. It was, thus, interesting to study the chemistry of the various Ir(tropp) complexes differing by the formal oxidation state of the metal centre with proton and hydride sources, and hydrogen. In *Scheme 1*, proton- (steps *c* and *d*) or hydride-transfer reactions (step *g*) to produce Ir(tropp) hydrides are represented.

We begin our syntheses by a simple reduction of the mixture of *trans*- and *cis*-isomers of the 16-electron complex $[Ir(tropp^{ph})_2]^+$ **2** with alkali metals M^1 = Li, Na, K, and the burgundy red iridate **4** is obtained in very good yield. As an isolated intermediate, the deep green 17-electron complex $[Ir(tropp^{ph})_2]$ **3** is formed (*Scheme 1*, *a* and *b*). Note that the *trans*- and *cis*-isomers of **2** do not inerconvert on the NMR time scale in noncoordinating or weakly coordinating solvents, while a dynamic equilibrium between the *trans*- and *cis*-isomers was established for **3** [43]. The d^{10}-valence-electron-configured iridate **4** shows a strongly distorted structure with the two P-atoms in *cis*-position. Also, we have no indications that the 17-electron or 18-electron complexes **3** or **4** form pentavalent 19-electron or 20-electron complexes, respectively. On the contrary, the cationic 16-electron complexes *trans*-**2** and *cis*-**2** form pentavalent complexes like **7a–c** (*Scheme 1*,*f*), and, as expected, these are intermediates on the path for the conversions: *trans*-$[Ir(tropp^{ph})_2]^+ + L \rightleftharpoons [Ir(L)(tropp^{ph})_2]^+ \rightleftharpoons$ *cis*-$Ir(tropp^{Ph})_2]^+ + L$. Finally, we have not observed yet that the tropp^{ph} ligand in **2**, **3**, or **4** can be displaced under usual conditions by another ligand meaning that tropp^{ph} is a quite effective chelate.

The 16-electron complex $[Ir(tropp^{ph})_2]^+$ **2** is not protonated even when exposed to an excess of a (perfluoroalkane)sulfonic acid for several days. When **4** is treated with exactly 1 equiv. of a strong acid (*i.e.*, $HBF_4 \cdot OEt_2$, $HO_3SC_4F_9$, HO_2CCF_3) or with an excess of AcOEt or H_2O, the monohydride $[IrH(tropp^{ph})_2]$ **5** forms quantitatively and was isolated as colorless crystals (*Scheme 1*,*c*). A *doublet* in the off-resonance ^{1}H-decoupled ^{31}P-NMR spectrum (δ 73.3) and a *triplet* for the hydride signal in the low-

Scheme 1. *Reactions of* **2**–**4** *with Proton and Hydride Sources to Give Hydrides* **5** *and* **6**

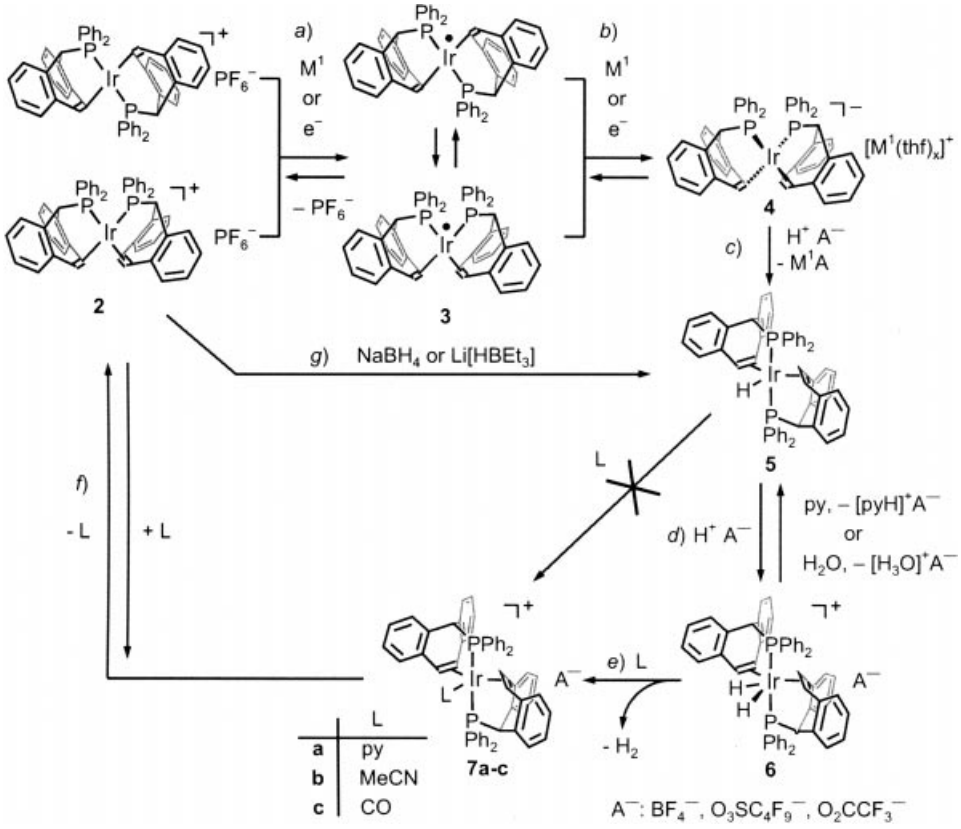

frequency region of the ^{1}H-NMR spectrum (δ −12.21, ^2J(P,H) = 16.3 Hz) establishes its formation. The Ir–H stretching mode in the IR spectrum ($\tilde{\nu}$ 2004 cm^{-1}) is observed in the typical range. Two signals are observed in the ^{1}H- and ^{13}C-NMR spectra for the olefinic H-atom and C-nuclei indicating that these are pair-wise nonequivalent. This finding is in accord with a structure in which the olefinic groups are bonded in the equatorial positions of a trigonal bipyramid or in the basal positions of a square pyramid, *i.e.*, two protons pointing to the 'inside' and two to the 'outside' of the coordination spheres (*Fig. 2*).

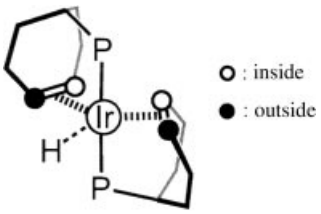

Fig. 2. *Denotation of 'inside' and 'outside' protons in trigonal bipyramidal [IrH(tropp^{ph})$_2$]* **5**

The monohydride is further protonated to give the cationic dihydride $[IrH_2(tropp^{ph})_2]^+$ **6** by an excess of strong acids such as $HBF_4 \cdot OEt_2$, $HO_3SC_4F_9$, or HO_2CCF_3 (*Scheme 1*, *d*), although the reaction with the latter is already quite slow. The formation and structure of **6** is corroborated by its off-resonance ^{1}H-decoupled ^{31}P-NMR (*triplet*, δ 61.3) and ^{1}H-NMR spectrum showing a *triplet* at $\delta -12.66$ ($^2J(P,H) = 11.8$) for the hydride. The ^{1}H resonances for the 'inside' and 'outside' olefinic H-atoms (*multiplet*, δ 5.31) were not resolved, but the nonequivalent olefinic ^{13}C-nuclei were observed (δ 82.7, 83.9). In the IR spectrum, the Ir–H stretching modes $\tilde{\nu}_{sym}$ and $\tilde{\nu}_{asym}$ are not separated, and only one absorption band typical for transition metal hydrides is observed at $\tilde{\nu}$ 2172 cm^{-1}. In an NMR experiment, we used the deuterated acid DO_2CCF_3 to produce the mixed hydride/deuteride $[IrDH(tropp^{ph})_2]^+$ d_1-**6**. In the ^{1}H-NMR spectrum, we find the hydride signal with half intensity and no ^{1}H,D coupling (*i.e.*, $J(D,H) < 2$ Hz). Also the measurement of the spin-lattice relaxation time T_1 (335 ms) gave no indication for the presence of a nonclassical dihydrogen complex $[Ir(H_2)(tropp^{ph})_2]^+$, for which T_1 is expected to be smaller than 100 ms at 300 MHz [44][45]. We assume, therefore, that the classical dihydride **6** is at least 10 kJ/mol lower in energy than the non-classical complex. However, for longer times, **6** is only stable under an atmosphere of H_2, otherwise the solution or even crystals become red, indicating the reductive elimination of H_2 from colorless **6** to red **2**. Both, the structures of **5** and **6**, were determined by X-ray analyses (*vide infra*), which confirm the conclusions drawn from the NMR data.

Upon treatment with pyridine (py), deprotonation of the dihydride **6** takes place instantaneously and the monohydride **5** is formed quantitatively (reverse of reaction *d* in *Scheme 1*). However, when the reaction solutions are kept at room temperature, slowly the formation of the cationic pentavalent 18-electron complex **7a** (L = py) is observed (after 4 d *ca.* 80%). When the dihydride **6** is dissolved in CH_2Cl_2/THF/H_2O 1:1:2 (*v*/*v*/*v*), *ca.* 58% **6** and 42% **5** are detected by ^{31}P-NMR spectroscopy. Also, several resonances of low intensity were recorded, but none of these signals could be assigned yet. Rapid displacement of H_2 was not observed, and, only after several days, the signals for the *trans*-**2** and *cis*-**2** appear. In a control experiment, no reaction between the tetracoordinated 16-electron complex **2** and H_2O was observed, which indicates that H_2O is a too weak ligand to form the complex $[Ir(H_2O)(tropp^{ph})_2]^+$. With a starting concentration of c_0 (**6**) = 0.023M and the concentrations given above for **6** and **5** in the equilibrium $[IrH_2(tropp^{ph})_2]^+ + H_2O \rightleftarrows [IrH(tropp^{ph})_2] + H_3O^+$, a p$K_s$ of *ca.* 2 results for **6**, which is in the expected range of *Brønstedt* acidity of dihydrides (for a review, see [46]).

Dihydrogen is easily displaced in a very clean reaction by weakly basic and small two-electron-donor ligands like MeCN and CO. Indeed, this reaction is so effective that vivid H_2 gas evolution is observed, when crystals of **6** are carefully covered with MeCN. Products of these reactions are exclusively the pentacoordinated species **7b**,**c** which were completely characterized by NMR spectroscopy. Characteristic for the trigonal bipyramidal structures of these complexes are the signals of the 'inside' and 'outside' protons in the ^{1}H-NMR spectrum. Since especially **7b**, which is labile and in equilibrium with **2**, can be reduced at rather low potentials [47], the reactions *a*–*f* in *Scheme 1* represent the complete set of chemical steps that would be involved in the reaction $H_2O + 2e^- \rightarrow H_2 + 2\ OH^-$ catalyzed by the Ir(tropp) complexes. This reaction

may become interesting, when an efficient way can be found to use photons as energy source and an inexpensive sacrificial electron donor (such as SO_2 or S_8) [7].

Very convenient ways to produce the monohydride **5** are the hydride-transfer reactions outlined in *Step g* of *Scheme 1*. Thus, the reaction of the cationic complexes **2** with either $NaBH_4$ or $Na(BHEt_3)$ was used to synthesize **5** in almost quantitative yield on a preparative scale. The monohydride **5** is stable and does not react with any of the ligands L (py, H_2O, MeCN, CO, and D_2) used in this work.

In this context, it was also interesting to study the reaction of the paramagnetic complex **3** with protic agents. Reaction of **3** with an excess of CF_3COOH causes an immediate color change from green to pale yellow, and, in the ^{31}P-NMR spectrum, the sharp resonance of the dihydride **6** and a broad signal at δ *ca.* 49 ppm was observed. The latter is assigned to the trifluoroacteate complex $[Ir(O_2CCF_3)(tropp^{ph})_2]$, which is in a dynamic equilibrium with the ionic form $[Ir(tropp^{ph})_2]^+ (O_2CCF_3)^-$. In accord with this assumption, the peak at δ 49 ppm disappears completely, when the solution is shaken under an atmosphere of H_2 for *ca.* 2 min, and only the signal for **6** is detected. The results of the reaction of **3** with H_2O are shown in *Scheme 2*.

Scheme 2. *Reaction of* **3** *with* H_2O *to Give Hydride* **5** *and Hydroxide* **8**

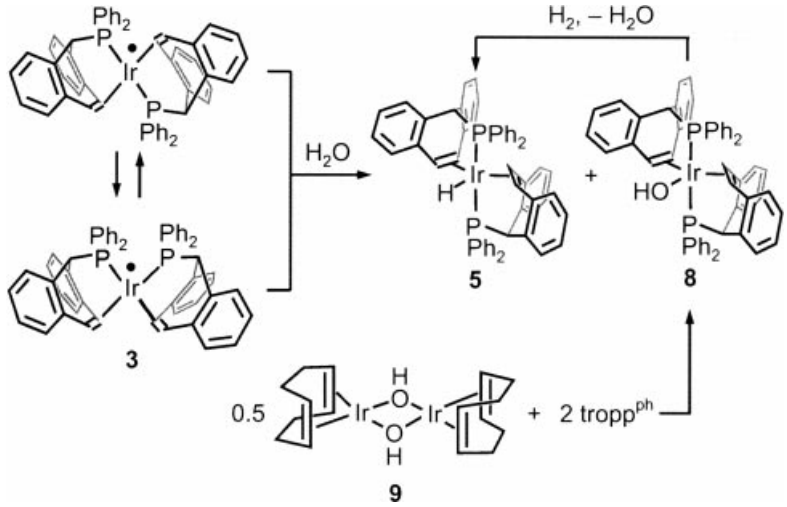

Adding a drop of H_2O to a deep green THF solution of **3** (*ca.* 20 mg in 0.6 ml of solvent) leads to an immediate fading of the green color, and a ^{31}P-NMR spectrum of the pale yellow solution recorded after *ca.* 2 min shows, apart from the signal of **5**, only one other signal at δ 48.8 ppm. The suspicion that this signal stems from the hydroxide **8** was confirmed by an independent synthesis. Using the hydroxide-bridged dimer $[Ir_2(\mu_2\text{-}OH)_2(cod)_2]$ [48] as precursor, reaction with 4 equiv. of $tropp^{ph}$ almost quantitatively yields **8**. Although we cannot definitively exclude that **8** is a dimer in which the Ir-centres are bridged by OH groups, the spectroscopic data, mass spectrometry, and steric considerations make a monomer with a terminal OH group more likely. When the hydroxide complex **8** is placed under an atmosphere of H_2 (1 atm.), a slow but clean reaction occurs, and, after *ca.* 2 h, the monohydride **5** is the sole product observed by

^{31}P- and ^{1}H-NMR spectroscopy. A probable mechanism for this reaction will be discussed below.

The mechanisms for the reaction of a paramagnetic 17-electron complex with H–X bonds are not straightforward and have been discussed controversially. For C–H activation reactions with the Rh^0 complex $[Rh(dppe)_2]$, *Eisenberg* and co-workers suggested an H-atom abstraction as initial step: $[Rh(dppe)_2] + H-X \rightarrow [RhH(dppe)_2] + X^{\cdot}$ (X = alkyl group) [2]. Subsequently, the generated $X^{\cdot}$ radical is then either reduced by $[Rh(dppe)_2]$ to X^-, which would be the expected reaction for X = OH, or rearranges to further products. However, in later work it was reported that $[Rh(dppe)_2]$ is not reactive with protic and H-atom sources [49].

On the other hand, in studies with the $[M(CO)(PPh_3)_3]$ system, abbreviated here as $[M^0]$ (M = Rh, Ir), *Pilloni* and co-workers favor a proton transfer as the initial step of the following sequence *1.1–1.3* [20]:

$$[M^0] + H_2O \rightleftharpoons [M^{II}-H]^+ + OH^- \quad (1.1)$$

$$[M^{II}-H]^+ + [M^0] \rightarrow [M^I-H] + [M^I]^+ \quad (1.2)$$

$$[M^I]^+ + OH^- \rightarrow [M^I-OH] \quad (1.3)$$

in order to explain the formally homolytic cleavage of H_2O in the reaction $2\,[M^0] + H_2O \rightarrow [M^I-H] + [M^I-OH]$. Related mechanisms have been proposed to account for the net reaction: $2\,[M^0] + MeCN \rightarrow [M^I-H] + [M^I-CH_2CN]$ [2][20]. Note in this context, that both the $[Ir(tropp^{ph})_2]$ **3** and the $[Ir(tropp^{ph})_2]^-$ **4** complex do not react with MeCN.

We have no indication for the formation of a 17-electron cationic hydrido complex comparable to $[M^{II}-H]^+$ in *Step 1.1* of the *Pilloni* mechanism[3]). Instead, when we try to generate this complex electrochemically by oxidation of the monohydride $[IrH(tropp^{ph})_2]$ **5**, an irreversible oxidation wave at $E_{ox} = +0.26$ V is seen in the first scan in a cyclic voltammogram (*Fig. 3*).

In subsequent scans, the typical reversible redox curves of the cation $[Ir(tropp^{ph})_2]^+$ are detected [34]. This behavior can be explained by the decomposition of the oxidized hydride, the 17-electron Ir^{II} complex $[IrH(tropp^{ph})_2]^+$ **3-H**$^+$ according to: $[IrH(tropp^{ph})_2]^+$ **3-H**$^+ \rightarrow 0.5\ H_2^+$ $[Ir(tropp^{ph})_2]^+$ **2** (H_2 evolution from Rh^{II} hydrides is discussed in [51]). However, when we assume that **3-H**$^+$ would be reduced at a potential more anodic than the oxidation potential of **3** (−0.65 V) with a rate faster than the decomposition of **3-H**$^+$, the reaction **3-H**$^+$ + **3** → **5** + **2** corresponding to *Step 1.2* is still possible. If we take the decomposition reaction of **3-H**$^+$ into account (see *Reaction 2.3* below), the reaction scheme given above might be modified according to:

$$[Ir(tropp^{ph})_2]\ \mathbf{3} + H_2O \rightarrow [IrH(tropp^{ph})_2]^+\ \mathbf{3\text{-}H}^+ + OH^- \quad (2.1)$$

$$[IrH(tropp^{ph})_2]^+\ \mathbf{3\text{-}H}^+ + [Ir(tropp^{ph})_2]\ \mathbf{3} \rightarrow [IrH(tropp^{ph})_2]\ \mathbf{5} + [Ir(tropp^{ph})_2]^+\ \mathbf{2} \quad (2.2)$$

---

[3]) It was reported that the M^{II} complexes $[MH(CO)(PPh_3)_3]^+$ are reversibly formed on the time scale of the performed electrochemical experiments. These complexes have a reduction potential far more anodic than the oxidation potential of the $[M(CO)(PPh_3)_3]$ species, *i.e.*, *Reaction 1.2* is exothermic [50].

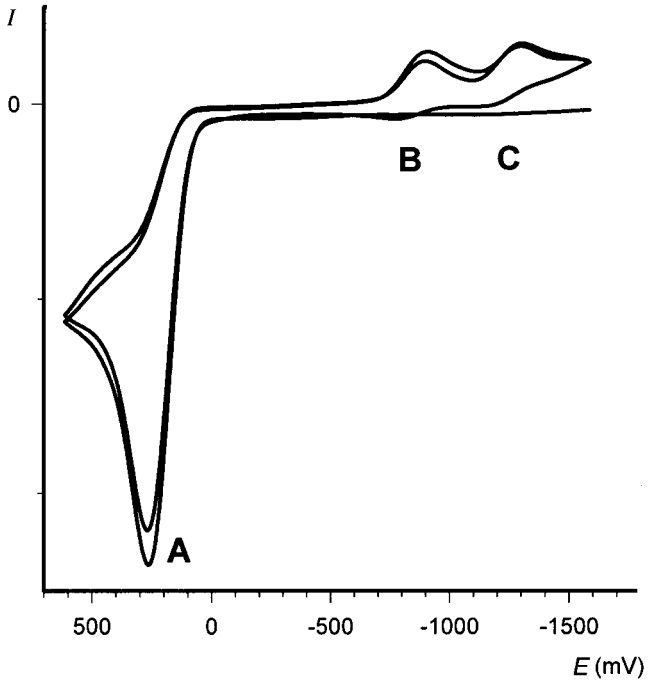

Fig. 3. *Cyclic voltammogram of [IrH(tropp^{ph})$_2$]* **5** *in THF/0.1*M*/Bu$_4$NPF$_6$ as electrolyte.* Scan rate: 100 mV·s^{-1}; $T = 298$ K. Potentials *vs.* Ag/AgCl, **A**: [IrH(tropp^{ph})$_2$]: E_{ox}(irrev) = +0.26 V; **B**: [Ir(tropp^{ph})$_2$]$^+$/[IrH(tropp^{ph})$_2$]: $E^1_{1/2} = -0.97$ V; **C**: [Ir(tropp^{ph})$_2$]/[IrH(tropp^{ph})$_2$]$^-$: $E^2_{1/2} = -1.43$ V.

$$[IrH(tropp^{ph})_2]^+ \textbf{3-H}^+ \rightarrow 0.5\ H_2 + [Ir(tropp^{ph})_2]^+ \textbf{2} \quad (2.3)$$

$$[Ir(tropp^{ph})_2]^+ \textbf{2} + OH^- \rightleftharpoons [IrOH(tropp^{ph})_2] \textbf{8} \quad (2.4)$$

$$H_2 + [Ir(tropp^{ph})_2]^+ \textbf{2} \rightarrow [IrH_2(tropp^{ph})_2]^+ \textbf{6} \quad (2.5)$$

$$[IrH_2(tropp^{ph})_2]^+ \textbf{6} + OH^- \rightarrow [IrH(tropp^{ph})_2] \textbf{5} + H_2O \quad (2.6)$$

The sequence of the *Reactions 2.3–2.6* make a straightforward likely mechanism for the net reaction of the hydroxide **8** with H_2 to give the monohydride **5** (see *Scheme 2*). However, since this reaction is overall slow, while addition of H_2 to **2** is fast, the equilibrium pointed out in *Reaction 2.4* must lie far to the right side, *i.e.*, the reaction rate for the formation of **8** is high. There is precedence for related reactions in the literature [52]. Under the assumption that **3** is easily protonated by H_2O, and that the electron-transfer *Reaction 2.2* is indeed faster than the decomposition (*Reaction 2.3*), the *Pilloni* mechanism including *Steps 2.1*, *2.2*, and *2.4* will be mainly responsible for the formation of **5** and **8** from the reaction of **3** with H_2O.

However, two other possibilities may be considered. The first is that actually the anionic complex $[M^{-I}]^-$ serves as the deprotonating agent, even when only present in very small amounts in the equilibrium of the disproportionation, 2 [Ir(tropp^{ph})$_2$]

(**3**) ⇌ [Ir(tropp^{ph})$_2$]$^+$ (**2**) + [Ir(tropp^{ph})$_2$]$^-$ (**4**) ($K_{disp} = 2.7 \cdot 10^{-5}$) (see also the discussion in [49]), while the cationic complex combines with OH^-. Hence, complex **3** is not directly involved in the reaction with H_2O.

The second possibility also accounting for the reaction of **3** with H_2O is the following sequence:

$$[Ir(tropp^{ph})_2]\ \mathbf{3} + H_2O \rightleftharpoons 2\ [IrH(OH)(tropp^{ph})_2]\ \mathbf{8\text{-}H} \quad (3.1)$$

$$[IrH(OH)(tropp^{ph})_2]\ \mathbf{8\text{-}H} + [Ir(tropp^{ph})_2]\ \mathbf{3} \rightarrow [IrH(OH)(tropp^{ph})_2]^+\ \mathbf{8\text{-}H}^+ + [Ir(tropp^{ph})_2]^-\ \mathbf{4} \quad (3.2)$$

$$[Ir(tropp^{ph})_2]^-\ \mathbf{4} + [IrH(OH)(tropp^{ph})_2]^+\ \mathbf{8\text{-}H} \rightarrow [IrH(tropp^{ph})_2]\ \mathbf{5} + [Ir(OH)(tropp^{ph})_2]\ \mathbf{8} \quad (3.3)$$

In this mechanism, the 19-electron Ir^{II} complex [IrH(OH)(tropp^{ph})$_2$] **8-H** is formed as the high-energy species either by direct oxidative addition of H_2O to the 17-electron Ir^0 complex **3** or by nucleophilic attack of OH^- on the Ir^{II} hydrido complex [IrH(tropp^{ph})$_2$]$^+$ **3-H**$^+$ (see protonation of **3** in *Reaction 2.1*). Since **8-H** should have a reduction potential far more cathodic than [Ir(tropp^{ph})$_2$], the redox reaction shown in *Reaction 3.2* will occur readily. Subsequently, [Ir(tropp^{ph})$_2$]$^-$ may deprotonate the acidic Ir^{III} complex [IrH(OH)(tropp^{ph})$_2$]$^+$ **8-H**$^+$ to give the final products (*Reaction 3.3*). In accord with this proposition are the observations that the dihydride [IrH$_2$(tropp^{ph})$_2$]$^+$ **6**, which is to some extent comparable to **8-H**$^+$, reacts with **4** to give 2 equiv. of **5** (*vide infra*), and that the reduction of [IrH$_2$(tropp^{ph})$_2$]$^+$ **6** to give the 19-electron species [IrH$_2$(tropp^{ph})$_2$] occurs irreversibly at negative potentials ($E_{red} < -2.0$ V *vs.* Ag/AgCl). However, a strong argument against this mechanism is that the intermediate [IrH(OH)(tropp^{ph})$_2$]$^+$ **8-H**$^+$ is not stable. Attempts to prepare **8-H**$^+$ by adding an acid to the slightly yellow solution of hydroxide complex [IrH(OH)-(tropp^{ph})$_2$] **8** led instantaneously to a red color, indicating the elimination of H_2O, [IrH(OH)(tropp^{ph})$_2$]$^+ \rightarrow$ [Ir(tropp^{ph})$_2$]$^+$ (**2**) + H_2O, and, in the ^{31}P-NMR spectrum, only the signal for **2** is observed, indeed.

Although, for the moment there is no definitive answer to the question for the mechanism of the formally simple reaction of **3** with H_2O, it is clear that it may be quite complex.

Reactions with Dihydrogen. The Ir complexes **2**–**4** varying only by their formal valence electron count from 16 to 18 were reacted with *ca.* 1 atmosphere of H_2. The results of these investigations are shown in *Scheme 3*.

The reaction with the tetracoordinated 16-electron complex **2** is a classical oxidative addition of H_2 to a tetracoordinated Ir^I centre, and, in a rapid exothermic reaction, the dihydride **6** is obtained in quantitative yield. As was already mentioned above, colorless **6** is stable for longer times only under an atmosphere of H_2, otherwise slow reductive elimination of H_2 to red **2** takes place. Because we assume that a nonclassical dihydrogen complex is an intermediate on this reaction path, which might have a structure closer to the tetracoordinated cation **2** than to the dihydride **6**, we exposed finely crushed microcrystalline **2** to a stream of H_2. Rapidly the red color disappeared, and a colorless product was formed. The solid-state ^{31}P-NMR spectrum (*Fig. 4*, top) of

Scheme 3. *Reactions of* **2**, **3**, *and* **4** *with* H_2

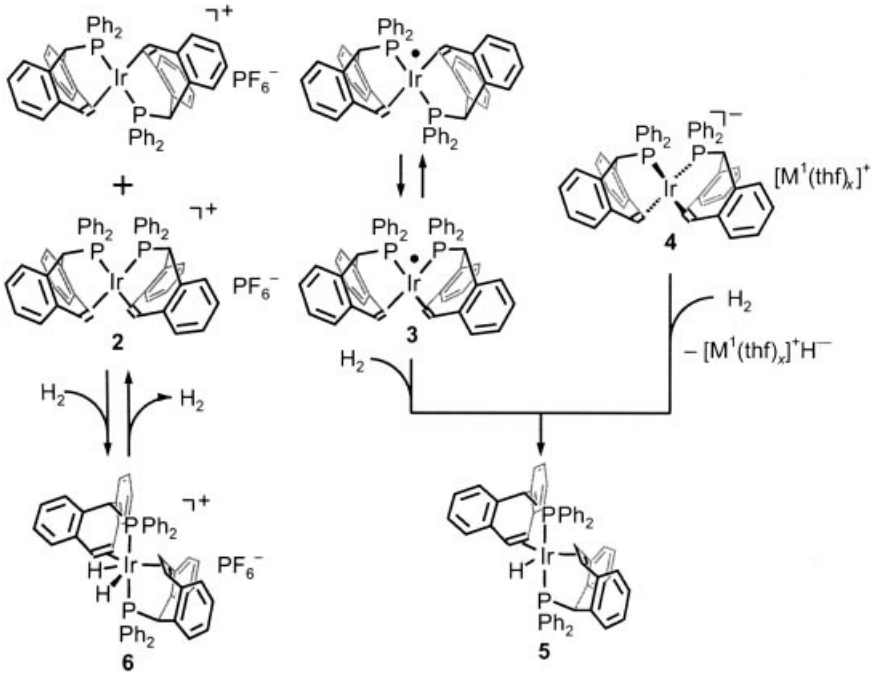

this product shows a relatively sharp septet for the $[PF_6]^-$ anion, a broad set of isotropic resonances centred at *ca.* 60 ppm, and a chemical-shift anisotropy-spinning side-band pattern consistent with the assigned structure as $[IrH_2(tropp^{ph})_2][PF_6]$.

The broadness of the latter features arises from the superposition of various sharper lines due to the presence of individual conformers as a consequence of the employed solid-gas preparation method. The solid-state ^{2}H-NMR spectrum (*Fig. 4*, bottom) shows a quadrupolar tensor close to axial symmetry, which is typically encountered in situations where the principal axis coincides with the M–D bond [53][54]. The absence of D,D dipolar coupling suggests furthermore that the two deuterons in the complex are relatively distant, contrary to what would have been expected for a nonclassical hydrogen complex [44][45]. Although this experiment was disappointing in the sense that such a complex could not be observed, it confirms our notion that the classical dihydride is thermodynamically considerably more stable.

The odd-electron complex $[Ir(tropp^{ph})_2]$ **3** reacts also very rapidly and quantitatively with H_2 to give the monohydride complex $[IrH(tropp^{ph})_2]$ **5**. The complex **5** does not exchange the H-centre against D under a D_2 atmosphere, indicating its inertness. Visually, the reaction of **3** with H_2 can be easily followed, and the deep green THF solution of **3** (*ca.* 0.03M) turns colorless within less than 2 min. Comparable reactions are known for quite some time and have been reported for the complexes $[Rh(dppe)_2]$ [22] and $[M(CO)(PPh_3)_3]$ [20], and mentioned in a footnote in ref. [22] for $[Rh\{P(O^iPr)_3\}_4]$ [25]. H_2 Cleavage has also been observed with Rh^{II}-Rh^{II} porphyrin dimers [51][55] and Co^{II} complexes like $[Co(CN)_5]^{3-}$ [56]. To our knowledge, no details about the mechanism (for a review on some general trends concerning the

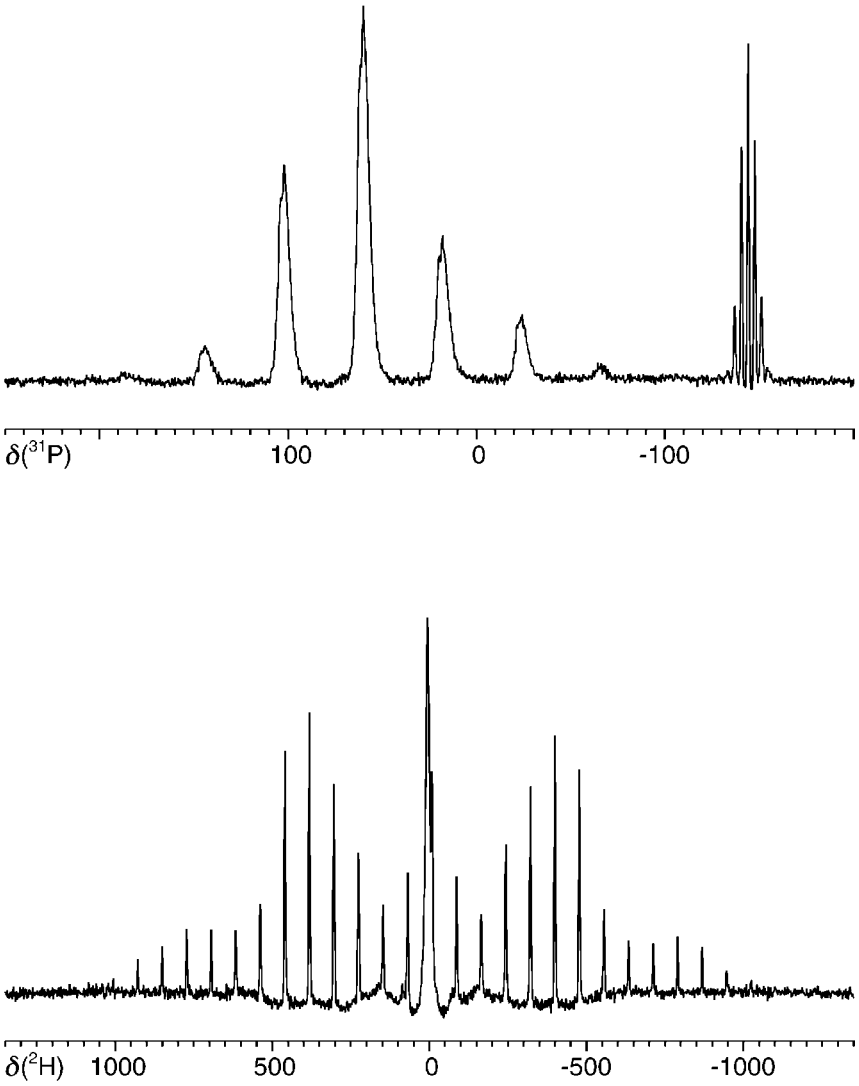

Fig. 4. *^{31}P-CP-MAS* (top) *and ^{2}H-MAS* (bottom) *NMR spectra of the solid-gas reaction product of [Ir(tropp^{ph})$_2$][PF$_6$] and H$_2$*. The spectra are consistent with the formation of [IrH(tropp^{ph})$_2$][PF$_6$] and the 'classical', *i.e.*, hydridic nature of the H ligands.

reactivity of open-shell organometallics see [57]) of this reaction were communicated, but we note that, apart from [Rh{P(O^{i}Pr)$_3$}$_4$], dimeric species have been detected in all these systems. Since, in our system, dimers can be definitively excluded[4]), one may

[4]) In a thorough EPR study [43], we observe exclusively the *cis*- and *trans*-isomers of **3** down to a temperature of 30 K, while the signal intensity remains unchanged. Note that for other systems, *i.e.*, [Rh(dppe)$_2$] and [Rh(CO)(PPh$_3$)$_3$] dimers are formed.

speculate about a mechanism that was already evoked to explain the reaction of **3** with H_2O (see *Reactions 3.1–3.3* above), *i.e.*, in a first reversible step, H_2 adds oxidatively to **3** under formation of the 19-electron Ir^{II} complex $[IrH_2(tropp^{ph})_2]$ (*Reaction 4.1*) which reduces unreacted **3** to **4** (*Reaction 4.2*), and finally proton exchange in an acid-base reaction takes place (*Reaction 4.3*) to give the final products:

$$[Ir(tropp^{ph})_2]\ \mathbf{3} + H_2 \rightleftharpoons [IrH_2(tropp^{ph})_2]\ \mathbf{3\text{-}H_2} \tag{4.1}$$

$$[IrH_2(tropp^{ph})_2]\ \mathbf{3\text{-}H_2} + [Ir(tropp^{ph})_2]\ \mathbf{3} \rightarrow [IrH_2(tropp^{ph})_2]^+\ \mathbf{6} + [Ir(tropp^{ph})_2]^-\ \mathbf{4} \tag{4.2}$$

$$[IrH_2(tropp^{ph})_2]^+\ \mathbf{6} + [Ir(tropp^{ph})_2]^-\ \mathbf{4} \rightarrow 2\ [IrH(tropp^{ph})_2]\ \mathbf{5} \tag{4.3}$$

A further possibility is, that the 19-electron species $\mathbf{3\text{-}H_2}$ transfers an H-atom either to the solvent or to **3** whereby also the monohydride complex **5** is formed (*4.4*):

$$[IrH_2(tropp^{ph})_2]\ \mathbf{3\text{-}H_2} \rightarrow [IrH(tropp^{ph})_2]\ \mathbf{5} + H^{\cdot} \tag{4.4}$$

The non-stability of the 19-electron dihydride $\mathbf{3\text{-}H_2}$ was already established by the cyclic voltammetry experiments mentioned above.

However, all these speculations are further complicated by the following experiment. When a frozen (D_8)THF solution of the salt $[Li(thf)_4]^+$ $[Ir(tropp^{ph})_2]^-$ **4** containing the electronically saturated 18-electron iridate anion is brought in contact with an atmosphere of H_2, a reaction is indicated by a color change from burgundy red to brownish-green as soon as the THF starts to melt. After *ca.* 5 min at room temperature, the solution has a red-brown color, and in the ^{31}P-NMR spectrum two signals, one at δ 45.7 (*ca.* 70%) and one at δ 72.1 ppm (*ca.* 30%), are detected. The latter signal stems from the monohydride **5** in this solvent. The formation of **5** is also clearly established by the observation of the corresponding hydride signal in the ^{1}H-NMR spectrum (a *triplet* at δ −12.3 ppm). After 10 min, the ^{31}P-NMR spectrum shows both signals in a 1:1 ratio, and, after 15 h, the monohydride **5** is present in *ca.* 90% apart from some signals with lower intensity. Also in the ^{1}H-NMR spectrum, apart from the major resonance of **5**, several signals in the hydride region (*i.e.*, δ −2 to −12) are observed. At the same time, a fine colorless powder is deposited on the bottom of the flask. When a drop of H_2O is added, H_2 evolution is observed, and the precipitate dissolves. Although further investigations are certainly needed, we suppose the deposit to be most likely $LiH(thf)_x$.

Unfortunately, we have not been able to characterize the first intermediate at δ 45.7 ppm in the reaction of **4** with H_2, but we believe it could be an aggregate of iridium monohydride **5** and lithium hydride of the type, $[IrLi(\mu_2\text{-}H)_2(tropp^{ph})_2(thf)_x]$ [58], from which $LiH(thf)_x$ starts to precipitate. This surprising reaction of **4** with H_2 formally corresponds to a two-electron reduction of H_2 to give 1 equiv. of a transition-metal hydride containing a covalently bonded hydride and 1 equiv. of a hydride salt. Such a reaction has, to our knowledge, not yet been reported for rhodates or iridates of the type $[ML_4]^-$. With respect to the reaction of the 17-electron Ir^0 complex **3** with H_2 to give hydride **5**, this finding adds another reaction sequence, which can be summarized as follows:

$$2\ [Ir(tropp^{ph})_2]\ \mathbf{3} \rightleftharpoons [Ir(tropp^{ph})_2]^+\ \mathbf{2} + [Ir(tropp^{ph})_2]^-\ \mathbf{4}\ (K_{disp} = 2.7 \cdot 10^{-5}) \quad (5.1)$$

$$[Ir(tropp^{ph})_2]^+\ \mathbf{2} + H_2 \rightleftharpoons [IrH_2(tropp^{ph})_2]^+\ \mathbf{6} \quad (5.2)$$

$$[Ir(tropp^{ph})_2]^-\ \mathbf{4} + H_2 \rightarrow [IrH(tropp^{ph})_2]\ \mathbf{5} + H^- \quad (5.3)$$

$$[IrH_2(tropp^{ph})_2]^+\ \mathbf{6} + H^- \rightarrow [IrH(tropp^{ph})_2]\ \mathbf{5} + H_2 \quad (5.4)$$

Note that in this reaction scheme – which we actually believe to be quite likely – the odd-electron species **3** is again not directly involved in the reaction with H_2.

Having investigated the reactions of **2**–**4** with proton sources and H_2, we also looked in a preliminary form at the reactions of these complexes with the hydrides **5** and **6**. These reactions were simply performed by mixing solutions of equimolar amounts of the reactants in NMR tubes. As expected, the cationic 16-electron Ir^I complex $[Ir(tropp^{ph})_2]^+$ **2** does not react with the monohydride $[IrH(tropp^{ph})_2]$ **5** nor with the dihydride $[IrH_2(tropp^{ph})_2]^+$ **6**. Also the Ir^0 complex $[Ir(tropp^{ph})_2]$ **3** does not react with **5**. The color of the THF solution remains green, and in the ^{31}P-NMR spectrum only **5** can be detected. However, **3** reacts rapidly with the dihydride **6** under formation of the monohydride **5** and the cation **2**. This reaction is complicated by the fact that the hydrides are not well-soluble in THF. On the other hand, in CH_2Cl_2, where **5** and **6** dissolve readily, the Ir^0 complex decomposes to yet unknown products. As was already mentioned above (see *Reaction 4.3*), the anion $[Ir(tropp^{ph})_2]^-$ **4** reacts with the dihydride **6** within 5 min to give in a clean acid-base reaction the monohydride **5**, which is unreactive towards **4**.

Structures of **5** *and* **6**. The structures of the monohydride $[IrH(tropp^{ph})_2]$ **5** and the dihydride $[IrH_2(tropp^{ph})_2]^+PF_6^-$ **6** were determined by X-ray analyses and are shown in *Figs. 5* and *6*. Selected bond lengths and angles are compiled in *Tables 1* and *2*.

The hydrides were not found in the *Fourier* map and are shown in assumed positions. In both Ir complexes, the P-atoms are *trans*-oriented and occupy the axial positions in the coordination polyhedra, and the olefins are in the equatorial plane. The

Table 1. *Selected Bond Lengths* [Å] *and Angles* [°] *for* **5**

Ir(1)–P(1)	2.2921(12)	C(5A)–Ir(1)–C(4)	92.66(15)
Ir(1)–P(2)	2.2878(12)	C(5A)–Ir(1)–C(4A)	38.89(15)
Ir(1)–C(4)	2.173(4)	C(4)–Ir(1)–C(4A)	131.55(15)
Ir(1)–C(5)	2.195(4)	C(5A)–Ir(1)–C(5)	131.17(15)
Ir(1)–C(4A)	2.168(4)	C(4)–Ir(1)–C(5)	38.51(14)
Ir(1)–C(5A)	2.179(4)	C(4A)–Ir(1)–C(5)	170.06(15)
P(1)–C(1)	1.873(4)	C(5A)–Ir(1)–P(2)	90.40(11)
P(1)–C(16)	1.835(4)	C(4)–Ir(1)–P(2)	94.82(11)
P(1)–C(22)	1.830(4)	C(4A)–Ir(1)–P(2)	87.60(11)
P(2)–C(1A)	1.867(4)	C(5)–Ir(1)–P(2)	93.46(11)
P(2)–C(16A)	1.832(4)	C(5A)–Ir(1)–P(1)	94.48(11)
P(2)–C(22A)	1.825(4)	C(4)–Ir(1)–P(1)	90.41(10)
C(4A)–C(5A)	1.447(6)	C(4A)–Ir(1)–P(1)	92.78(11)
C(4)–C(5)	1.441(5)	C(5)–Ir(1)–P(1)	87.44(11)
		P(2)–Ir(1)–P(1)	172.67(3)

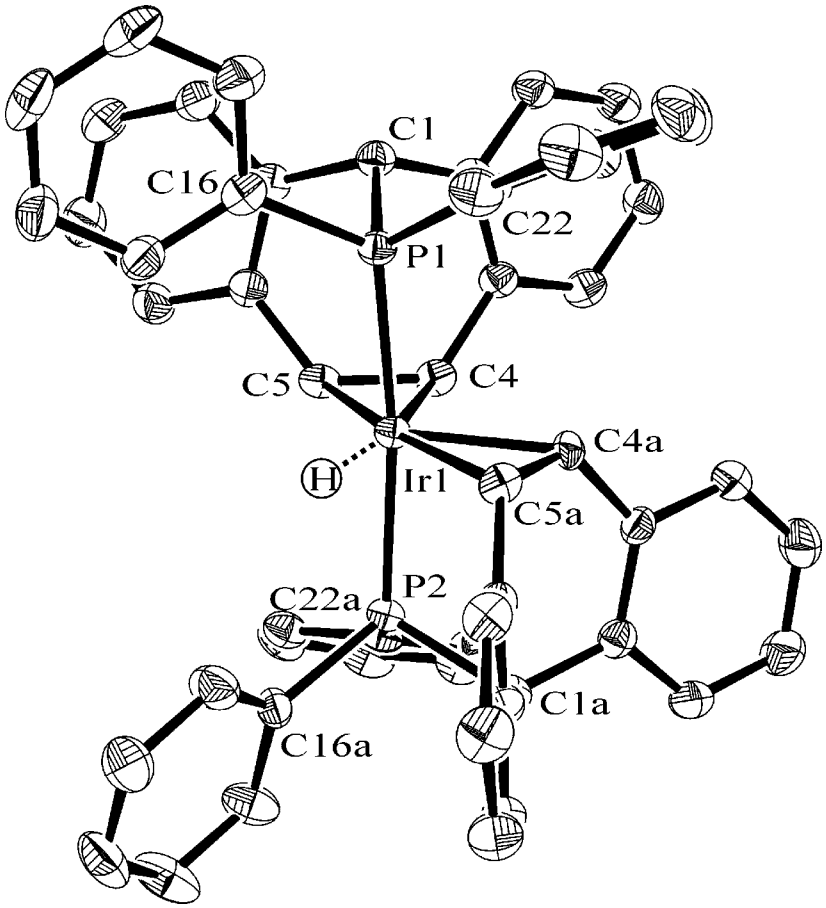

Fig. 5. *Molecular structure of [IrH(tropp^{ph})$_2$]* **5**. H-Atoms were omitted for clarity. Selected bond lengths and angles are given in *Table 1*.

Table 2. *Selected Bond Lengths* [Å] *and Angles* [°] *for* **6**

Ir(1)–P(1)	2.300(6)	C(4A)–Ir(1)–C(4)	144.4(8)
Ir(1)–P(1A)	2.329(5)	C(4A)–Ir(1)–P(1)	96.0(6)
Ir(1)–C(4)	2.30(2)	C(4)–Ir(1)–P(1)	86.5(5)
Ir(1)–C(5)	2.443(19)	C(4A)–Ir(1)–P(1A)	88.3(5)
Ir(1)–C(4A)	2.29(2)	C(4)–Ir(1)–P(1A)	95.1(5)
Ir(1)–C(5A)	2.46(3)	P(1)–Ir(1)–P(1A)	170.3(2)
P(1)–C(1)	1.85(2)	C(4A)–Ir(1)–C(5)	109.2(7)
P(1)–C(16)	1.79(2)	C(4)–Ir(1)–C(5)	35.2(7)
P(1)–C(22)	1.85(2)	P(1)–Ir(1)–C(5)	88.1(5)
P(1A)–C(1A)	1.859(18)	P(1A)–Ir(1)–C(5)	98.7(5)
P(1A)–C(16A)	1.80(2)	C(4A)–Ir(1)–C(5A)	35.8(7)
P(1A)–C(22A)	1.92(2)	C(4)–Ir(1)–C(5A)	108.6(8)
C(4)–C(5)	1.44(3)	P(1)–Ir(1)–C(5A)	98.6(6)
C(4A)–C(5A)	1.47(3)	P(1A)–Ir(1)–C(5A)	90.0(6)
		C(5)–Ir(1)–C(5A)	73.6(8)

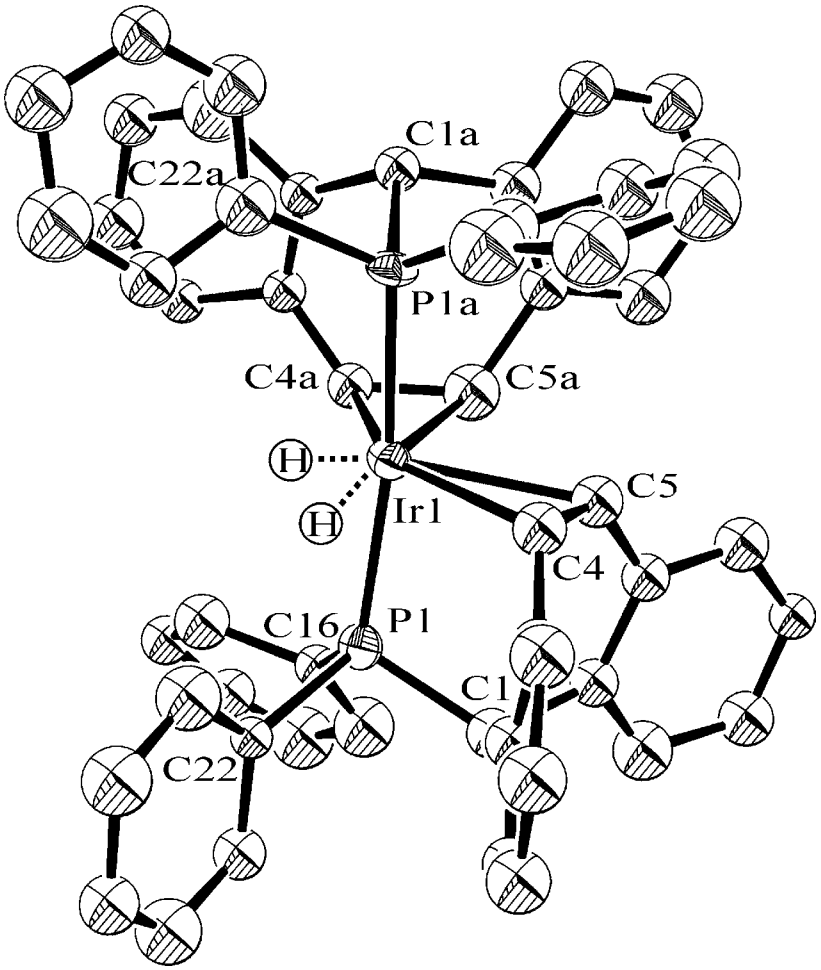

Fig. 6. *Molecular structure of* $[IrH_2(tropp^{ph})_2]^+$ **6**. The PF_6^- counter anion and the H-atoms were omitted for clarity. Selected bond lengths and angles are given in *Table 2*.

averaged Ir–P bond lengths (**5**: 2.29 Å; **6**: 2.31 Å) lie within the range observed in comparable compounds [59] and, as expected, are slightly longer (*ca.* 0.02 Å) in the hexacoordinated complex **6**. Significant differences show the Ir–C distances in the monohydride **5** (average 2.18 Å) and the dihydride **6** (average 2.37 Å). These bonds are much longer (0.2 Å) in **6**, and these structural data become apparent in the ^{13}C-NMR data (*vide infra*). On the other hand, the lengths of the coordinated olefins (1.44–1.47 Å) in **5** and **6** do not vary much, and are slightly longer than in the cation **2** (1.42 Å) and close to the ones in the anion **4** (1.47 Å).

It is instructive at this point to compare the ^{13}C chemical shifts of the olefinic C-atoms in the cationic Ir^{I} complex **2**, the anionic Ir^{-I} complex **4**, the Ir^{I} monohydride **5**, and the cationic Ir^{III} dihydride complex **6** (*Table 3*).

Table 3. *^{13}C-NMR Chemical Shifts (δ vs. $SiMe_4$) of the Olefinic C-Atoms of the tropp Ligands in* **2**, **4**, **5**, *and* **6**

	δ (^{13}C(1))	δ (^{13}C(2))
$[Ir(tropp^{ph})_2]^+$ **2**	68.9	68.9[a])
$[Ir(tropp^{ph})_2]^-$ **4**	44.7	44.2
$[IrH(tropp^{ph})_2]$ **5**	36.8	34.7
$[IrH_2(tropp^{ph})_2]^+$ **6**	83.9	82.7

[a]) Only the chemical shift of the *trans*-isomer (88%) is given.

Frequently, ^{13}C-NMR chemical shifts are used to assign a more olefinic (high-frequency shifts, large δ values) or more cyclopropane character (low-frequency shifts, small δ values) to a coordinated olefin [60]. Applying this criterion to the various $[Ir(tropp^{ph})_2]$ complexes listed in *Table 3*, the monohydride complex **5** shows the highest iridacyclopropane character in its bonds towards the olefins. Interestingly, these resonances are even more low-frequency-shifted than in the iridate **4** despite the formal -1 oxidation state of the Ir-centre in the latter. This may be interpreted in terms of the particularly high electron donation from the hydride ligand that also binds in the equatorial plane and renders the metal centre electron-rich (and, hence, a high degree of metal-to-ligand π-back bonding and metallacyclopropane character results). Note, however, that the ^{13}C olefin resonances of the iridate anion **4** are shifted to lower frequencies by more than 20 ppm when compared to the cationic Ir^I complex **2**, which indicates that a considerable amount of electron density is shifted from the metal to the ligand in **4**. As expected, the corresponding ^{13}C olefin resonances in the complex **6** are the most deshielded. Applying the classical *Dewar-Chatt-Duncanson* bond model, this is expected in view of the formal $+3$ oxidation state of the Ir-atom indicating that π-back-bonding is less than in the remaining complexes shown in *Table 3*.

Conclusion. – The Ir(tropp) complexes $[Ir(tropp^{ph})_2]^n$ (**2**: $n=+1$, **3**: $n=0$, **4**: $n=-1$) can be isolated in pure form and, thus, especially for the odd-electron species **3**, allowed to study their reactions with protic reagents and H_2, which are the crucial steps in catalytic cycles designed for H_2 evolution from protic media. A further advantage of these tropp complexes is that the metal centre resides in a rigid coordination sphere so that ligand-exchange processes are minimized, which are otherwise frequently observed in electron-rich complexes where metal ligand anti-bonding orbitals are occupied. The reactions which have been described in this work are summarized in *Scheme 4*.

While the cationic 16-electron complexes *trans*-**2** and *cis*-**2** react neither with H_2O nor with strong proton sources, the neutral 17-electron complex **3** and anionic 18-electron complex **4** react with H_2O and acids. As product, the very stable Ir^I monohydride complex $[IrH(tropp^{ph})_2]$ **5** is obtained. In reactions with **3**, the hydroxide $[Ir(OH)(tropp^{ph})_2]$ **8** is formed in equal amounts. Stronger acids protonate **5**, and the cationic dihydride Ir^{III} complex $[IrH_2(tropp^{ph})_2]^+$ **6** is obtained. Addition of a base like pyridine or H_2O deprotonates **6** (partially with H_2O) to give **5**, and, after longer reaction times, either the pentavalent complex $[Ir(py)(tropp^{ph})_2]^+$ **7a** or the tetracoordinated Ir complex **2** (in reactions with H_2O) is obtained. Indeed, hydrogen loss from **6** is easily induced by other small two-electron donor ligands like MeCN and CO, and the complexes $[Ir(L)(tropp^{ph})_2]^+$ with L = MeCN **7b** or L = CO **7c** form quantitatively.

Scheme 4. *Summary of the Reactions of* **2**–**8**. Reactions with protic reagents are indicated with filled arrows, those with H_2 with unfilled arrows.

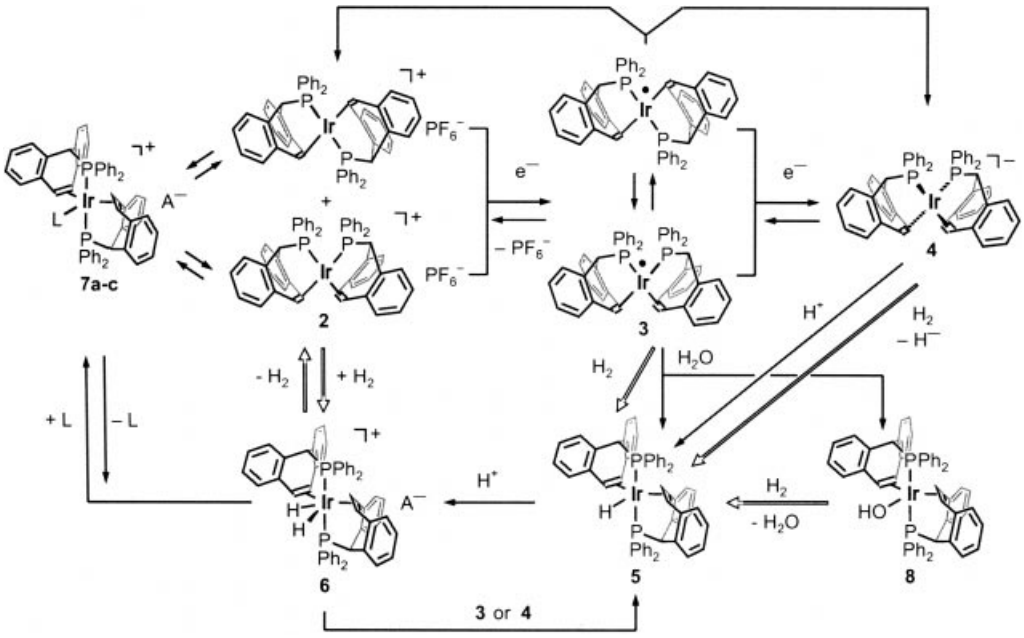

The Ir(tropp)complexes **2**–**4**, and **8** react with H_2. The monohydride **5** is inert. While the reaction with $[Ir(tropp^{ph})_2]^+$ **2** is a classical oxidative addition, and the reaction of $[Ir(OH)(tropp^{ph})_2]$ **8** can be assumed to proceed *via* the pre-equilibrium $\mathbf{8} \rightleftharpoons \mathbf{2} + OH^-$, the reactions of **3** and **4** are less evident. This is especially true for reactions with the odd-electron species **3** for which, however, the disproportionation, $2\,\mathbf{3} \rightleftharpoons \mathbf{2} + \mathbf{4}$, has to be taken into account. The diamagnetic species **2** and **4** may be actually the reactive species, *i.e.*, the reactions, *a*) $2\,\mathbf{3} + H_2O \rightarrow \mathbf{5} + \mathbf{8}$, and, *b*) $2\,\mathbf{3} + H_2 \rightarrow 2\,\mathbf{5}$, may actually include mechanisms involving the steps, $\mathbf{4} + H_2O \rightarrow \mathbf{5} + OH^-$ and $\mathbf{2} + OH^- \rightarrow \mathbf{8}$ for *a*, and $\mathbf{2} + H_2 \rightarrow \mathbf{6}$ and $\mathbf{6} + \mathbf{4} \rightarrow 2\,\mathbf{5}$ for *b*. After all, one is left with the puzzling situation that all species involved in the disproportion react with H_2, each one with a different rate, to give products that further react among each other. At this point, it is unclear whether the paramagnetic 17-electron complex $[Ir(tropp^{ph})_2]$ **3** is directly involved in any of the reactions with proton sources or H_2. Careful kinetic investigations of this rather complex reaction scheme would be necessary; however, our attempts were complicated by constraints imposed by exact dosage and determination of H_2 contents in organic solvents.

Certainly the most interesting finding in this work is that the electronically saturated 18-electron iridate $[Ir(tropp^{ph})_2]^-$ **4** also reacts readily with H_2, whereby ultimately the monohydride $[IrH(tropp^{ph})_2]$ **5** and an ionic hydride is formed. If a way can be found to transform **5** back to **2** (*i.e.*, by making synthetic use of the Ir–H bond in **5**), a low-energy electrocatalytic way for the formally simple reaction $H_2 + 2e^- \rightarrow 2\,H^-$ may be found with Ir(tropp)-type complexes as catalysts. This goal may be achieved by a suitable functionalization of the tropp system.

Experimental Part

General. All manipulations were carried out by standard *Schlenk* and glove-box techniques under purified Ar. Solvents were degassed and dried using standard procedures. The ligand 5-(diphenylphosphanyl)-5*H*-dibenzo[*a*,*d*]cycloheptene ($tropp^{ph}$) **1** [33] and the complexes $[Ir(tropp^{ph})_2]PF_6$ **2**, $[Ir(tropp^{ph})_2]$ **3**, $[Li(thf)_4]^+[Ir(tropp^{ph})_2]^-$ **4** [36], and $[Ir_2(\mu_2\text{-}OH)_2(cod)_2]$ **9** [48] were synthesized according to literature methods. All other reagents were used as supplied. UV/VIS Spectra: *Perkin-Elmer* UV/VIS/NIR spectrometer *Lambda-19*. IR Spectra ($\tilde{\nu}$ in cm^{-1}): *Perkin-Elmer* FT-IR spectrometer *2000*. NMR: *Bruker DPX-Avance-Series* 250–400 MHz. ^{1}H- and ^{13}C-chemical shifts are calibrated against the solvent signal ($CDCl_3$: ^{1}H-NMR: 7.27 ppm; ^{13}C-NMR: 77.2 ppm; CD_2Cl_2: ^{1}H-NMR: 5.32 ppm; ^{13}C-NMR: 54.0 ppm; CD_3CN: ^{1}H-NMR: 1.98 ppm; ^{13}C-NMR: 117.8); ^{31}P chemical shifts are calibrated against 85% H_3PO_4 as external standard. All NMR spectra were measured at r.t. In the following, we list selected characteristic spectroscopic data. Full data sets can be obtained from the authors upon request.

Solid-State NMR Spectroscopy: ^{31}P- and ^{2}H-NMR spectra were measured on a *Bruker Avance-500* spectrometer operating at 202.4 and 76.7 MHz, resp. Magic-angle spinning and, for ^{31}P, cross-polarization techniques were employed. Reported ^{31}P chemical shifts are given relative to $(NH_4)H_2PO_4$.

Cyclic voltammograms were measured with an *EG & G* potentiostat model *362* with a Pt working electrode (∅0.785 mm^2), a Pt counter electrode, and an Ag reference electrode. After each measurement, ferrocene (fc) was added as internal standard, and the potential of the redox couple fc/fc^+ was set to +0.352 V *vs.* Ag/AgCl.

*Bis[5-(diphenylphosphanyl)-5*H*-dibenzo[*a,d*]cyclohepten]iridium(I) Hydride* ($[IrH(tropp^{ph})_2]$; **5**). To a soln. of 109 mg of $[Ir(tropp^{ph})_2]PF_6$ **2** (0.1 mmol) in 3 ml of THF, 102 µl of a 1M THF soln. of $LiHBEt_3$ (0.011 mmol) was added slowly at r.t. The red soln. became colorless after 2 min. The solvents were removed in vacuum, and the residue was dissolved in CH_2Cl_2 and filtered. Slow evaporation of the solvent gave **5** (92 mg, 95%) as a colorless micro-crystalline product. Recrystallization from a CH_2Cl_2/Et_2O 1:2 gave suitable crystals for an X-ray analysis. M.p. 171–174° (dec.). IR: 2004*m* (Ir–H). ^{1}H-NMR (CD_2Cl_2): 5.32 (*t*, *J*(P,H) = 3.2, 2 CHP); 3.06 (*m*, 2 =CH); 2.73 (*m*, 2 = CH); −12.21 (*t*, *J*(P,H) = 16.3, IrH). ^{13}C-NMR (CD_2Cl_2): 50.6 (*t*, *J*(P,C) = 11.9, 2 CHP); 36.8 (*s*, 2 =CH); 34.7 (*s*, 2 =CH). ^{31}P-NMR (CD_2Cl_2): 73.3. Anal. calc. for $C_{54}H_{43}IrP_2$: C 68.86, H 4.54; found: C 68.53, H 4.34.

*Bis[5-(diphenylphosphanyl)-5*H*-dibenzo[*a,d*]cyclohepten]iridium(III) Dihydride Hexafluorophosphate* ($[Ir(H_2)(tropp^{ph})_2]PF_6$, **6**. A soln. of 109 mg of $[Ir(tropp^{ph})_2]PF_6$ **2** (0.1 mmol) in CH_2Cl_2 was flushed with H_2. The red soln. became immediately colorless. The product was precipitated with hexane. Evaporation of the solvents gave 98 mg (90%) of **6**. The dihydride **6** can be stored under an atmosphere of H_2. Recrystallization from a CH_2Cl_2/hexane 1:1 gave colorless crystals suitable for an X-ray analysis. IR: 2172*m* (Ir–H). ^{1}H-NMR (CD_2Cl_2): 5.63 (*t*, *J*(P,H) = 3.6, 2 CHP); 5.31 (*m*, 4 =CH); −12.66 (*t*, *J*(P,H) = 11.8, IrH_2). ^{13}C-NMR (CD_2Cl_2): 83.9 (*s*, 2 =CH); 82.7 (*s*, 2 =CH); 52.6 (*t*, *J*(P,C) = 12.0, 2 CHP). ^{31}P-NMR (CD_2Cl_2): 61.3, −143.1 (PF_6). Anal. calc. for $C_{54}H_{44}F_6IrP_3$: C 59.39, H 4.22; found: C 58.97, H 4.09.

*Bis[5-(diphenylphosphanyl)-5*H*-dibenzo[*a,d*]cyclohepten](pyridine)iridium hexafluorophosphate* ($[Ir(py)(tropp^{ph})_2]PF_6$, **7a**). To a soln. of 109 mg of $[Ir(tropp^{ph})_2]PF_6$ (**2**) (0.1 mmol) in 5 ml of CH_2Cl_2 an excess of pyridine was added *via* a syringe. The soln. became colorless after 5 min. The solvents were removed in vacuum and, after recrystallization from CH_2Cl_2/hexane 1:4, 107 mg of **7a** (92%) were obtained as a white microcrystalline prowder. M.p. 131–135° (dec.). ^{1}H-NMR (CD_2Cl_2): 8.72 (br. *s*, 2 H–C(2) of py); 5.47 (*t*, *J*(P,H) = 3.7, 2 CHP); 4.32 (*m*, 2 =CH); 3.91 (*m*, 2 =CH). ^{13}C-NMR (CD_2Cl_2): 155.1 (*s*, 2 C, C(1) of py), 48.7 (*s*, 2 =CH); 48.5 (*t*, *J*(P,C) = 12.1, 2 CHP); 46.3 (*s*, 2 =CH). ^{31}P-NMR (CD_2Cl_2): 48.6, −143.1 (PF_6). Anal. calc. for $C_{59}H_{47}F_6IrNOP_3$: C 60.56, H 4.02, N 1.19; found: C 59.98, H 3.94, N 1.12.

*(Acetonitrile)bis[5-(diphenylphosphanyl)-5*H*-dibenzo[*a,d*]cyclohepten]iridium(I) Hexafluorophosphate* ($[Ir(MeCN)(tropp^{ph})_2]PF_6$, **7b**). To a soln. of 109 mg of $[Ir(tropp^{ph})_2]PF_6$ (**2**) (0.1 mmol) in 5 ml of CH_2Cl_2, an excess of MeCN was added *via* a syringe. The soln. became colorless after 5 min, and subsequently the solvents were removed in vacuum. After recrystallization from a CH_2Cl_2/hexane 1:3, 108 mg **9a** (96%) were obtained as a white microcrystalline powder. M.p. 167–170° (dec.). ^{1}H-NMR (CD_3CN): 5.71 (*t*, *J*(P,H) = 3.7, 2 CHP); 4.12 (*m*, 4 =CH). ^{13}C-NMR (CD_3CN): 48.1 (*s*, 2 =CH); 47.2 (*s*, 2 =CH); 46.7 (*t*, *J*(P,C) = 13.9, 2 CHP). ^{31}P-NMR (CD_3CN): 52.7 − 142.1 (PF_6). Anal. calc. for $C_{56}H_{45}F_6IrNP_3$: C 59.41, H 3.98, N 1.24; found: C 59.22, H 3.76, N 1.01.

*(Carbonyl)bis[5-(diphenylphosphanyl)-5*H*-dibenzo[*a,d*]cyclohepten]iridium Hexafluorophosphate* ($[Ir(CO)(tropp^{ph})_2]PF_6$, **7c**). A soln. of 109 mg of $[Ir(tropp^{ph})_2]PF_6$ (**2**) (0.1 mmol) in CH_2Cl_2 was flushed with CO gas. The red soln. became immediately colorless. The product was precipitated with hexane and washed several times with hexane. Evaporation of the solvents gave 92 mg of **7c** (95%). M.p. 110–114° (dec.). IR: 1861*m*

(CO). ^{1}H-NMR ($CDCl_3$): 5.59 (t, J(P,H) = 4.1, 2 CHP); 4.54 (m, 2 =CH); 3.62 (m, 2 =CH). ^{13}C-NMR ($CDCl_3$): 174.8 (t, J(P,C) = 11.0, CO); 61.3 (s, 2 =CH); 61.0 (s, 2 =CH); 49.9 (t, J(P,C) = 12.1, 2 CHP). ^{31}P-NMR ($CDCl_3$): 53.9 – 143.3 (PF_6). Anal. calc. for $C_{55}H_{42}F_6IrOP_3$: C 59.03, H 3.73; found: C 58.74, H 3.53.

*Bis[5-(diphenylphosphanyl)-5*H*-dibenzo[*a,d*]cyclohepten]iridium(I) Hydroxide* ([Ir(OH)(tropp^{ph})$_2$], **8**). To a soln. of 63 mg of [Ir$_2$(μ_2-OH)$_2$(cod)$_2$] **9** (0.1 mmol) in 3 ml of THF, a soln. of 151 mg of tropp^{ph} (0.4 mmol) in 3 ml of THF was slowly added at r.t. The mixture was stirred for *ca*. 30 min, and, subsequently, the solvent was removed in vacuum. The residue was washed with hexane leaving 152 mg **7** (79%) as a white powder. M.p. 168 – 171° (dec.). ^{1}H-NMR (CD_2Cl_2): 5.29 (t, J(P,H) = 3.5, 2 CHP); 4.24 (m, 2 =CH); 3.84 (m, 2 =CH) 1.68 (br. s, OH). ^{13}C-NMR (CD_2Cl_2): 49.9 (t, J(P,C) = 12.8, 2 CHP); 47.9 (s, 2 =CH); 43.0 (s, 2 =CH). ^{31}P-NMR (CD_2Cl_2): 48.8. Anal. calc. for $C_{54}H_{43}IrOP_2$: C 67.35, H 4.47; found: C 67.03, H 4.40.

X-Ray Crystal Structure Analyses. Details of the data collection are given in *Table 4*.

Table 4. *Crystal Data for [IrH(tropp^{ph})$_2$]* **5** *and [IrH$_2$(tropp^{ph})$_2$]PF$_6$* **6**

	5	**6**
Formula	$C_{61}H_{51}IrOP_2$	$C_{54}H_{42}Cl_{2.50}F_6IrP_3$
Formula weight	1054.16	1178.61
Crystal system	Triclinic	Monoclinic
Space group	*P*1	*P*2
Wavelength [Å]	0.71073	0.71073
Temp. [K]	173(2)	233(2)
a [Å]	9.5470(19)	23.3175(6)
b [Å]	13.394(3)	19.5473(6)
c [Å]	19.356(4)	12.0105(3)
α [°]	97.74(3)	90
β [°]	102.10(3)	97.9910(10)
γ [°]	99.52(3)	90
Z, D_x [Mg/m^3]	2, 1.490	4, 1.444
V [A^3]	2349.7(8)	5421.2(3)
Absorption coefficient [mm^{-1}]	2.952	2.729
F(000)	1064	2338
Crystal size [mm]	0.71 × 0.62 × 0.54	0.52 × 0.37 × 0.29
Reflections collected/unique	21575/8917	15593/6867
R(int)	0.0360	0.1255
Data/restraints/parameters	8917/0/562	6867/10/303
R_1, wR_2 [$I > 2\sigma(I)$]	0.0308, 0.0820	0.0654, 0.1542
R_1, wR_2 (all data)	0.0335, 0.0907	0.0965, 0.1711

The structure of **5** was measured on a *STOE Image* plate, solved using direct methods and was refined against the full matrix (*vs.* F^2) with SHELXTL (Version 5.0) [62]. Non-H-atoms were treated anisotropically, H-atoms were refined on calculated positions using the riding model. One noncoordinating solvent molecule was refined with isotropic temp. factors. The structure **6** was measured on a *Siemens SMART PLATFORM* with CCD Detector, solved using direct methods, and was refined against the full matrix (*vs.* F^2) with SHELXTL (Version 5.0) [61]. Heavy-atoms were treated anisotropically, C-atoms were treated isotropically. H-Atoms were refined on calculated positions with the riding model. The PF_6 anion was refined as rigid group being disordered over several positions. Noncoordinating solvent molecules were refined with isotropic temp. factors. An absorption correction was not applied.

Crystallographic data (excluding structure factors) for the structures reported in this paper have been deposited with the *Cambridge Crystallographic Data Centre* as supplementary publication No. CCDC-163558 (**5**) and CCDC-163559 (**6**). Copies of the data can be obtained, free of charge, on application to CCDC, 12 Union Road, Cambridge CB2 1EZ, UK (fax: (+44) 1223-336-033; e-mail: deposit@ccdc.cam.ac.uk).

This work was supported by the *Swiss National Science Foundation.*

REFERENCES

[1] HiChun Kang, C. H. Mauldin, T. Cole, W. Slegeir, K. Cann, R. Pettit, *J. Am. Chem. Soc*. **1977**, *99*, 8323.
[2] J. A. Sofranko, R. Eisenberg, J. A. Kampmeier, *J. Am. Chem. Soc*. **1980**, *102*, 1163; J. A. Sofranko, R. Eisenberg, J. A. Kampmeier, *J. Am. Chem. Soc*. **1979**, *101*, 1042.
[3] S. Slater, J. H. Wagenknecht, *J. Am. Chem. Soc*. **1984**, *106*, 5367.
[4] A. Szymaszek, F. P. Pruchnik, *J. Organomet. Chem*. **1989**, *376*, 133, and refs. cit. therein.
[5] B. Bogdanović, W. Leitner, Ch. Six, U. Wilczok, K. Wittmann, *Angew. Chem.* **1997**, *109*, 518; *Angew. Chem., Int. Ed*. **1997**, *36*, 500, and refs. cit. therein.
[6] A. S. Chan, H.-S. Shieh, *Inorg. Chim. Acta* **1994**, *218*, 89, and refs. cit. therein.
[7] S. Oishi, *J. Mol. Catal*. **1987**, *39*, 225.
[8] A. J. L. Hanlan, G. A. Ozin, *Inorg. Chem*. **1979**, *18*, 2091, and refs. cit. therein.
[9] A. B. P. Lever, G. A. Ozin, A. J. L. Hanlan, W. J. Power, H. B. Gray, *Inorg. Chem*. **1979**, *18*, 2088.
[10] J. H. B. Chenier, M. Histed, J. A. Howard, H. A. Joly, H. Morris, B. Mile, *Inorg. Chem.* **1989**, *28*, 4114.
[11] P. Chini, S. Martinengo, *Inorg. Chim. Acta* **1969**, *3*, 21.
[12] L. Malatesta, G. Caglio, M. Angoletta, *J. Chem. Soc., Chem. Commun*. **1970**, 532.
[13] T. Kruck, N. Derner, W. Lang, *Z. Naturforsch., B* **1966**, *21*, 1020.
[14] M. A. Bennett, D. J. Patmore, *Inorg. Chem*. **1971**, *10*, 2387, and refs. cit. therein.
[15] D. A. Clement, J. F. Nixon, *J. Chem. Soc., Dalton Trans.* **1973**, 195.
[16] J. P. Collman, F. D. Vastine, W. R. Roper, *J. Am. Chem. Soc*. **1968**, *90*, 2282, and refs. cit. therein.
[17] G. G. Johnston, M. C. Baird, *J. Organomet. Chem*. **1986**, *314*, C51.
[18] B. Longato, L. Riello, G. Bandoli, G. Pilloni, *Inorg. Chem*. **1999**, *38*, 2818.
[19] N. Mézailles, P. Rosa, L. Ricard, F. Mathey, P. Le Floch, *Organometallics* **2000**, *19*, 2941.
[20] G. Zotti, S. Zecchin, G. Pilloni, *J. Organomet. Chem*. **1983**, *246*, 61.
[21] G. Zotti, S. Zecchin, G. Pilloni, *J. Electroanal. Chem*. **1984**, *175*, 241.
[22] K. T. Mueller, A. J. Kunin, S. Greiner, T. Henderson, R. W. Kreilick, R. Eisenberg, *J. Am. Chem. Soc*. **1987**, *109*, 6313, and refs. cit. therein.
[23] A. S. C. Chan, J. R. Hill, H. Sieh, *J. Chem. Soc., Chem. Commun*. **1983**, 688.
[24] A. S. C. Chan, H. Sieh, J. R. Hill, *J. Organomet. Chem.* **1985**, *279*, 171.
[25] G. George, S. Klein, J. Nixon, *Chem. Phys. Lett*. **1984**, *108*, 627.
[26] H. Căldăraru, K. de Armond, K. W. Hanck, V. Em Sahini, *J. Am. Chem. Soc*. **1976**, *98*, 4455.
[27] W. A. Fordyce, K. H. Pool, G. A. Crosby, *Inorg. Chem*. **1982**, *21*, 1027, and refs. cit. therein.
[28] C. Costa, C. Travagnacco, G. Balducci, G. Mestroni, G. Zassinovich, *J. Electronanal. Chem*. **1989**, *261*, 189.
[29] J. Orsini, W. E. Geiger, *J. Electroanal. Chem.* **1995**, *380*, 83.
[30] J. L. Vidal, W. E. Walker, *Inorg. Chem.* **1981**, *20*, 249.
[31] R. Whyman, *J. Chem. Soc., Chem. Commun.* **1969**, 1381.
[32] G. Pilloni, E. Vecchi, M. Martelli, *J. Electronanal. Chem.* **1973**, *45*, 483.
[33] J. Thomaier, S. Boulmaâz, H. Schönberg, H. Rüegger, A. Currao, H. Grützmacher, H. Hillebrecht, H. Pritzkow, *New J. Chem.* **1998**, *21*, 947.
[34] H. Schönberg, S. Boulmaâz, M. Wörle, L. Liesum, A. Schweiger, H. Grützmacher, *Angew. Chem*. **1998**, *109*, 1492; *Angew. Chem., Int. Ed*. **1998**, *37*, 1423.
[35] S. Deblon, H. Rüegger, H. Schönberg, S. Loss, V. Gramlich, H. Grützmacher, *New. J. Chem*. **2001**, *25*, 83.
[36] H. Grützmacher, H. Schönberg, S. Boulmaâz, M. Mlakar, S. Deblon, S. Loss, M. Wörle, *J. Chem. Soc., Chem. Commun*. **1998**, 2623.
[37] D. S. Moore, S. D. Robinson, *Chem. Soc. Rev*. **1983**, *12*, 415.
[38] S. I. Murahashi, H. Takaya, *Acc. Chem. Res.* **2000**, *33*, 225.
[39] P. P. Deutsch, R. Eisenberg, *Chem. Rev.* **1988**, *88*, 1147.
[40] J. D. Atwood, *Coord. Chem. Rev.* **1988**, *83*, 93.
[41] R. H. Crabtree, H. Felkin, G. E. Morris, *J. Chem. Soc., Chem. Commun*. **1976**, 716.
[42] B. F. M. Kimmich, E. Somsook, C. R. Landis, *J. Am. Chem. Soc*. **1998**, *120*, 10115.
[43] S. Deblon, L. Liesum, J. Harmer, H. Schönberg, A. Schweiger, H. Grützmacher, *Chem. – Eur. J.* **2001**, in press.
[44] D. M. Heinekey, W. J. Oldham Jr., *Chem. Rev.* **1993**, *93*, 913.
[45] P. J. Desroisers, L. Cai, Z. Lin, R. Richards, J. Halpern, *J. Am. Chem. Soc.* **1991**, *113*, 4173.
[46] R. G. Pearson, *Chem. Rev.* **1985**, *85*, 41.
[47] M. Rudolph, M. Mlakar, S. Boulmaâz, H. Schönberg, H. Grützmacher, unpublished results.

[48] L. M. Green, D. W. Meek, *Organometallics* **1989**, *8*, 659.
[49] A. J. Kunin, E. J. Nanni, R. Eisenberg, *Inorg. Chem*. **1985**, *24*, 1852.
[50] G. Pilloni, G. Schiavon, G. Zotti, S. Zecchin, *J. Organomet. Chem.* **1977**, *134*, 305.
[51] V. Grass, D. Lexa, J.-M. Savéant, *J. Am. Chem. Soc*. **1997**, *119*, 7526, and refs. cit. therein.
[52] D. P. Paterniti, P. J. Roman, J. D. Atwood, *Organometallics* **1997**, *16*, 3371, and refs. cit. therein; J. S. Thompson, S. L. Randall, J. A. Atwood, *Organometallics* **1991**, *10*, 3906.
[53] V. I. Bakhmutov, C. Bianchini, F. Maseras, A. Lledos, M. Peruzzini, E. V. Vorontsov, *Chem. – Eur. J.* **1999**, *5*, 3318.
[54] G. Facey, D. Gusev, R. H. Morris, S. Macholl, G. Buntkowsky, *Phys. Chem. Chem. Phys.* **2000**, *2*, 935.
[55] B. B. Wayland, S. Ba, A. E. Sherry, *J. Am. Chem. Soc*. **1991**, *113*, 5305; B. B. Wayland, B. A. Woods, R. Pierce, *J. Am. Chem. Soc.* **1982**, *104*, 302.
[56] B. R. James, 'Homogeneous Hydrogenation', John Wiley & Sons, New York, 1973.
[57] R. Poli, *Chem. Rev.* **1996**, *96*, 2135.
[58] A. Albinati, L. M. Venanzi, *Coord. Chem. Rev*. **2000**, *200*, 687.
[59] A. G. Orpen, L. Brammer, F. H. Allen, O. Kennard, D. G. Watson, *J. Chem. Soc., Dalton Trans.* **1989**, S1.
[60] B. E. Mann, B. E. Taylor, '^{13}C-NMR Data for Organometallic Compounds', Academic Press, London, **1981**, 16.
[61] G. M. Sheldrick, *Acta Crystallogr., Sect. A* **1990**, *46*, 467; G. M. Sheldrick, SHELX 97; Universität Göttingen, Germany, 1997.

Received June 27, 2001